GU J Sci, Part C, 9(3): 463-477 (2021)

Gazi University

**Journal of Science**

PART C: DESIGN AND TECHNOLOGY

http://dergipark.gov.tr/gujsc

# Investigation of a Storage Type Solar-Driven Solid Desiccant Cooling System

Nima KHOSRAVI[1] Devrim AYDIN[1*]

[1]*Department of Mechanical Engineering, Eastern Mediterranean University, G. Magosa, TRNC, Mersin 10, Turkey*

***Article Info***

*Research article*
*Received:27/05/2021*
*Revision:12/07/2021*
*Accepted:26/07/2021*

**Keywords**

*Solid Desiccant*
*Coolth Storage*
*Evaporative Cooling*
*Solar Energy*
*Experimental*

**Abstract**

Solar-driven solid desiccant assisted evaporative cooling could be an effective alternative to conventional vapour compression cooling systems due to its lower operating costs and lower environmental impact. This technology has been widely investigated for continuous operation through the use of desiccant wheels. However, the investigation of such technology for storing solar radiation in the form of coolth energy is missing in the literature. In that regard, primary objective of the present study is to investigate a fixed bed solar driven desiccant assisted evaporative cooling system, that uses vermiculite-calcium chloride composite sorbent, to be utilized as a coolth storage in hot-humid climate. To achieve this aim, a prototype unit was designed, developed and tested under real climatic conditions of North Cyprus. According to the results, over six hours of charging period, at regeneration temperature between 51 – 62 °C and air mass flow rate of 0.03 kg/s, average moisture desorption rate of 3.9 g/min was obtained. On the other hand, over four hours of discharging at air inlet temperature of 32 – 35 °C and mass flow rate of 0.06 kg/s, vermiculite-calcium chloride / wood chips couple provided average air temperature drop and cooling capacity of 8.4 °C and 0.49 kW respectively. Hygrothermal efficiency of the system is also found 0.65. Additionally, the average wet-bulb effectiveness and average dew-point effectiveness were obtained as 121.6%, and 90.2% respectively. Furthermore average total and thermal coefficient of performance of 0.35 and 0.6 were achieved over the three consecutive cycles. These results suggest that the proposed system could be a potential technology for storing solar energy to be used in air conditioning applications in buildings.

## 1. INTRODUCTION

According to the International Institute of Refrigeration, 15% of the global electricity production is consumed for the refrigeration and air-conditioning. In addition, approximately 45% of the total energy consumed by the commercial buildings and residences is used for air-conditioning and the demand is increasing continuously [1]. Moreover, the concerns on the environmental impact of greenhouse gases are also increasing. Currently, conventional vapor compression based HVAC systems are widely used. However, these systems present some restrictions due to the environmental problems derived from the use of refrigerant gases and considerable energy consumption [2].

Desiccant assisted evaporative cooling (DAEC) has been regarded as an alternative residential air conditioning method, owing to its potential for considerably reducing electric power consumption. In particular, when DAEC system is combined with solar thermal collectors, it becomes an attractive sustainable air conditioning option, as in such configuration, the energy required for regeneration of the desiccant is supplied by solar energy [3].

Numerous experimental and mathematical studies have been previously conducted on desiccant cooling systems. Jagirdar et al. mathematically investigated an internally cooled and heated desiccant-coated heat-mass exchanger driven by low-grade heat [4]. According to the study results, cooling COP up to 9.8 and effectiveness value up to 0.88 is obtained. Jia et al. [5] analyzed an integrated rotary desiccant

*Corresponding author, e-mail: devrim.aydin@emu.edu.tr
DOI: 10.29109/gujsc.943429

dehumidifier-vapor compression air conditioning unit. They inferred that hybrid desiccant cooling can economize the electric power consumption up to 37.5% compared to a vapor compression refrigeration cycle. Asim et al. [6] present a critical study on the properties of adsorbent materials for desiccant cooling applications. The study focused on important factors such as environmental conditions, system design and costs. Jani et al. [7] proposed a hybrid solid desiccant vapor compression air-conditioning system for a hot and humid climate. Researchers concluded that the latent part of cooling load is considerably reduced by the integration of desiccant dehumidifier which enhances the performance of the cycle. Belguith et al. carried out a performance investigation of the impact of the ambient conditions on the desiccant cooling systems with cycle COP of 1.89 [8]. Aoul et al. investigated the feasibility of extending an existing solar thermal system in a school building in Abu Dhabi to provide dehumidification for the existing air conditioning system through a desiccant system. It was concluded that the system can remove 35% of the moisture from the air, simultaneously saving 10% of the building's energy [9]. Study of a novel dehumidification system based on silica gel packed beds is carried out by De Antonellis et al. [10]. Depending on bed thickness, airflow arrangement and air velocity, the humidity ratio of airflow supplied to the building can be increased from 1.5 g/kg to 4.8 - 5.8 g/kg when the indoor humidity ratio is 5.8 g/kg and the regeneration temperature is around 50 °C. Comino et al. [2] experimentally determined the seasonal coefficient of performance (SCOP) of a solar driven desiccant cooling system to control indoor conditions in a research lab room. The experimental results showed that the system independently adjusted the temperature and humidity of the supply air. 75% of the energy consumed by this air handling system comes from renewable sources. Hussain et al. [11] presented numerical investigations on a solar-assisted hybrid DAEC system integrated with solar air collectors for hot and humid climatic conditions of Kuwait. The outcomes of this work indicated that the proposed system is capable of providing average coefficient of performance of 0.85. Bleibel et al. investigated the performance of an integrated evaporatively-cooled window with a desiccant dehumidification system combined with a photovoltaic/thermal unit [12]. It was found that system reduces the inner window temperature up to 7 °C during summer period corresponding to 11% decrease of the total cooling load. In another research, Pandelidis et al. [13] presented a numerical study of a multi-stage desiccant A/C process designed for moderate climates. Maximum $COP_t$ of the investigated system was determined as 4. In different study, a solar-driven desiccant evaporative cooling system for air-conditioning was proposed, which converts solar heat energy into cooling with built-in daily storage and provided 122.86 kWh of cooling [14]. Kousar et al. [15] performed detailed techno-economic analysis for three different solar driven DAEC configurations. Maximum COP and energy efficiency ratio with direct EC in process and regeneration sides is achieved as 0.76 and 7.19 respectively. In another study, Heidari et al. [16] presented a DAEC system using silica gel for co-production of water and cooling. $COP_{avg}$ of the system was achieved as 1.53, whereas for the same operating conditions, COP for the VC system was found as 1.2. An integrated system to regenerate the desiccant materials in fixed bed filled with silica gel for solar A/C system applications was developed by Avargani et al. [17]. The regeneration rate of the desiccant material and the average daily thermal regeneration efficiency of the system were obtained as 0.4 kg water/$hm^2$ and 30%, respectively.

Taking into the account of the former researches in the literature, present study concerns with the design and development of a storage type solar driven solid desiccant assisted evaporative cooling (SD-SDAEC) system that could be utilized for air conditioning applications in hot-humid climates. In previous research of the authors, proposed DAEC process was tested in laboratory environment [18]. In present study, based on the obtained encouraging results in previous laboratory experiments, system is integrated with solar collectors and tested in real climate conditions. During the experiments, composite desiccant consisting of vermiculite and calcium chloride also wood chips as the evaporative cooling (EC) pad, which have been previously investigated by the authors, were utilized [18]. The developed system was tested to analyze the real-life implementation performance of SD-SDAEC for coolth energy storage in hot-humid climates. The study suggests an innovative integration method of the investigated process to the existing solar water heating systems in buildings. With the suggested method, the desiccant cooling system could be charged (desiccant dehumidification) with domestic solar water heaters (SWHs). As a result, coolth energy is stored within the SD-SDAEC system for later usage (i.e., night time cooling). In discharging (cooling) mode, the heat generated due to the moisture sorption could be rejected to the cold water tank, which is generally installed together with the existing SWH. The new contribution of this

study is to demonstrate a new storage type desiccant based air cooling process driven by solar energy. Also experimental investigation of such process under Mediterranean Climate is novel. The proposed integrated process consisting of solar water heater, air to water heat exchanger, fixed bed desiccant unit and fixed bed EC chamber is described and tested first time in the literature, and possible implementation of it in new and existing buildings could provide considerable energy and cost savings in A/c applications. Meanwhile, such applications could enhance the utility of existing solar water heating systems installed in buildings during the summer period.

## 2. MATERIALS AND METHODS

### 2.1. Process Design

In the present work, a storage type SD-SDAEC system was tested in North Cyprus and its thermal performance assessment is carried out. As discussed earlier, proposed system can be driven by low grade thermal energy, such as renewable energy sources (i.e. solar energy), which has a large energy saving potential. Based on the available literature, none of studies have been conducted on the designing of a SD-SDAEC system using Vmc-$CaCl_2$ as a desiccant material for coolth energy storage in hot and humid climate. The synthesize procedure of Vmc-$CaCl_2$ was previously described in [18]. The 2-Dimensional view of the designed SD-SDAEC system is presented in Figure 1. The proposed concept consists of a solar water heating system, desiccant chamber and the evaporative cooling chamber. It has a cyclic operation. In charging mode, water is heated passively by the solar collector (1) and the hot water is collected in a hot water storage tank (2). The tank is connected to a water to air heat exchanger with a pipeline where the hot water circulates in between (3-5). Simultaneously, ambient air (6) is blown across the heat exchanger with the use of a ducting fan (7) thereby its temperature increases (8) as a result of the heat transferred from the water. Hot air than passes across the solid desiccant bed and desorbs the moisture (9). Moist air at the exit of desiccant chamber is released to the environment. As a result of this process, desiccant material is dehumidified and it gets ready for the discharging (cooling) cycle. In discharging cycle, pump in the hot water tank-heat exchanger line is deactivated and there is no hot water circulation across the heat exchanger (3-5). Ambient air (6) is blown to the system with the fan (7), it passes through heat exchanger without any heat exchange (8) and it enters the desiccant chamber where moisture is removed, and dry air leaves the chamber (9). The sorption heat generated during this process is eliminated by using a heat exchanger at the exit of the desiccant chamber (10). With the heat exchanger, the sorption heat of the air is transferred to a water tank with the water circulation (11-13) and the air temperature is reduced back to nearly ambient temperature. Finally dry air enters the evaporative cooling chamber and its temperature is reduced to the desired level. Finally, cool air (24-25 °C) is obtained at the evaporative cooler outlet (14).

In order to measure the water temperature in solar collector line during the charging mode, a thermometer with four channels has been used (Please see: Points 1-4 in Figure 1). Moreover, two SHTC3 Sensiron type sensors were installed at points (8) and (9) to measure the inlet and outlet desiccant temperature and humidity. Also one sensor was installed at point (6) to measure the ambient temperature and humidity. A PASCO-GLX airflow meter was used to measure the airflow speed at the system outlet (9). During the charging process the Eppley Precision Spectral Pyranometer (PSP) was used for measuring the solar intensity on the solar collector. On the other hand, in discharging process temperature and humidity of ambient air (6), inlet-outlet of desiccant unit (8-9) also outlet of heat exchanger and evaporation chamber (10-14) were measured with the installed SHTC3 Sensiron type sensors. A PASCO-GLX airflow meter was used to measure the airflow speed at the outlet of the system (14). Also a thermometer has been used to measure the circulation water temperature (11-13) inside the water tank. The measurement ranges of utilized sensors and their accuracies were listed in Table 1.
In the system, a ducting fan (120 W max. power) was installed at point (6) for air supply to the process. In addition, a 100 W water pump was installed at point (4) to circulate water between storage tank and the heat exchanger.

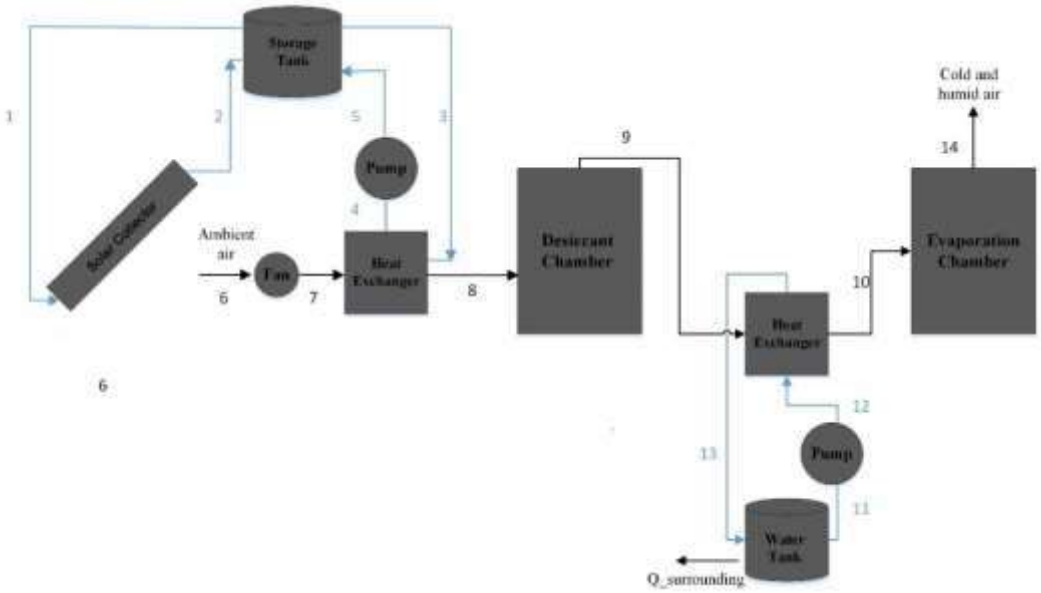


***Figure 1**. 2D view of the storage type SD-SDAEC system*

***Table 1.** Range and accuracy of the measurement devices*

| Sensor | Measured parameter | Range | Accuracy |
|---|---|---|---|
| Temperature (Sensirion-SHTC3) | Temperature | 0 – 130 ºC | ±0.2 ºC |
| Humidity (Sensirion-SHTC3) | Relative humidity | 0 – 100 % | ±2 % |
| Anemometer (Pasco-Xplorer) | Air velocity | 2 – 6 m/s | ±0.1 m/s |
| Temperature Data Logger | Temperature | -100 – 1370 °C | ±0.5 °C |
| Eppley Pyranometer (PSP) | Solar intensity | 0 – 2800 W/m$^2$ | ±3 W/m$^2$ |

A single glazing flat plate solar collector was designed and assembled in order to utilize the solar thermal energy in the charging process of the solar-driven DAEC system. Because of better characteristics like light weight, high strength, proper corrosion properties, high surface reflectivity, and good thermal conductivity, Aluminum flat plate was used in this study. The geometrical parameters and properties of the flat plate solar collector are given in Table 2.

***Table 2.** The geometrical data of the designed flat plate solar collector*

| **Item** | **Symbol** | **Value /Details** | **Unit** |
|---|---|---|---|
| Length | L | 1940 | mm |
| Height | H | 940 | mm |
| Width | w | 90 | mm |
| Collector weight | - | 24,5 | kg |
| Insulation | - | 50, special solar rock wool | mm |
| Collector glazing | - | 3.2, structured solar safety glass | mm |
| Conversion factor | $\eta_0$ | 0,78 | - |

## 2.2. Experimental Procedure

The operation of the SD-SDAEC system can be described with the “charging – discharging” cyclic order. The tests were performed between 30$^{th}$ July and 15$^{th}$ August of 2020. All the discharging tests were done during the evenings between 18:00 and 22:00 in outdoors; hence, solar heat had no effect on the discharging tests. In the discharging and charging processes, air mass flow rate of 0.06 kg/s and 0.03 kg/s were used respectively. Views of the manufactured and investigated SD-SDAEC system are presented in Figure 2 (a-b). During the experiments, air temperature and humidity were measured in both charging and

discharging cycles. Accordingly, heat transfer rates across the system components, solar collector efficiency, wet bulb and dry bulb effectiveness values, thermal and total COP, also water absorption/desorption rates and hygro-cyclic efficiency were determined.


***Figure 2.*** *Photographs of the designed SD-SDAEC system (a) front view and (b) rear view*

### 2.3. Governing Equations

The cooling capacity is determined via Equation (1) [19];

$$\dot{Q}_c = \dot{m}_a \Delta h = \dot{m}_a . C_p . (T_8 - T_{14}) \tag{1}$$

Air absolute humidity could be obtained with the following equation [20];

$$w = 216.7 \left[ \frac{\frac{RH}{100\%} 6.112 . exp\left(\frac{17.62.T}{243.12+T}\right)}{273.15+T} \right] \tag{2}$$

Dehumidification and humidification rate of air could be obtained by consideration of air humidity content difference across the desiccant and EC units [21] as illustrated in Equations (3) and (4) respectively;

$$\dot{m}_{dhum} = \dot{m}_a . (w_8 - w_9) \tag{3}$$

$$\dot{m}_{hum} = \dot{m}_a . (w_{14} - w_{10}) \tag{4}$$

The energy balance across the water-to-air heat exchanger could be written as;

$$\dot{m}_w . c_p . \left(T_{w,o} - T_{w,i}\right) = \dot{m}_a . c_p . (T_9 - T_{10}) \tag{5}$$

The wet-bulb ($\varepsilon_{wb}$) and dew point effectiveness ($\varepsilon_d$) of the process could be obtained via Equations (6) and (7) [22];

$$\varepsilon_{wb} = \frac{T_8 - T_{14}}{T_8 - T_{wb}} \tag{6}$$

$$\varepsilon_d = \frac{T_8 - T_{14}}{T_8 - T_d} \tag{7}$$

Where $T_8$ is equal to the system inlet (ambient) temperature ($T_6$), and $T_{14}$ is the system outlet temperature.

In charging cycle, $\dot{Q}_{solar,ava}$ represents the available solar energy on the collector surface and it could be calculated by multiplying the collector surface area ($A_{ap}$) with the solar irradiance ($I$), as given in Equation (8);

$$\dot{Q}_{solar,ava} = I . A_{ap} \tag{8}$$

The rate of heat gain $\left(\dot{Q}_{solar,g}\right)$ by the flat plate solar collector in charging cycles is calculated with the Equation (9):

$$\dot{Q}_{solar,g} = I.A_{ap}.\eta_{collector} \tag{9}$$

Where $\eta_{collector}$ could be calculated via Equation (10):

$$\eta_{collector} = \frac{\dot{m}_w.C_p.(T_1-T_2)}{A_{ap}.I} \tag{10}$$

Thermal ($COP_{th}$) and total performance ($COP_t$) coefficient of the system could be determined with Equations (11) and (12);

$$COP_{th} = \frac{\dot{Q}_c.t_{dc}}{\dot{Q}_{useful,Hx}.t_{cr}} \tag{11}$$

$$COP_t = \frac{\dot{Q}_c.t_{dc}}{E_i} \tag{12}$$

where, the nominator in both equations represents the produced total cooling in kJ, while the denominator in Equations (11) and (12) are; solar energy transfer to charging air (in kJ) and total energy consumption of system (thermal + electrical) in charging cycle.

Here, system's total energy consumption is calculated with Equation (13);

$$E_i = \left(\dot{W}_P + \dot{W}_f\right).(t_{dc}) + \left(\dot{W}_P + \dot{W}_f\right).(t_{cr}) + \dot{Q}_{useful,Hx}.(t_{cr}) \tag{13}$$

Useful rate of solar energy transferred to the charging air could be determined by obtaining the enthalpy change of air across the heat exchanger via Equation (14) where, mass flow rate of charging air is defined as $\dot{m}_a$, and enthalpy of air at inlet and outlet of heat exchanger is specified as $h_7$ and $h_8$, respectively.

$$\dot{Q}_{useful,Hx} = \dot{m}_a.(h_8 - h_7) \tag{14}$$

The heat transferred from the air to the desiccant across the desiccant chamber can be found by using Equation (15):

$$\dot{Q}_{trans,des} = \dot{m}_a.(h_8 - h_9) \tag{15}$$

where enthalpy at inlet and outlet of desiccant unit are specified as $h_8$ and $h_9$, respectively.

The charging efficiency $\left(\eta_{ch}\right)$ is defined as the ratio of the heat transfer across the desiccant chamber to the solar energy gained by collector as presented in Equation (16):

$$\eta_{ch} = \frac{\dot{Q}_{trans,des}}{\dot{Q}_{solar,g}} \tag{16}$$

The hygrothermal efficiency ($\eta_{hyg}$) is another important parameter that was analyzed in the study which is calculated by using Equation (17) as below:

$$\eta_{hyg} = \frac{m_{des}}{m_{abs}} \tag{17}$$

The overall uncertainty in calculation of the $\varepsilon_{wb}$ can be expressed as [23,24];

$$w_R = \left[\left(\frac{\partial \varepsilon_{wb}}{\partial T_1} w_{T_1}\right)^2 + \left(\frac{\partial \varepsilon_{wb}}{\partial T_4} w_{T_4}\right)^2 + \left(\frac{\partial \varepsilon_{wb}}{\partial RH_4} w_{RH_4}\right)^2\right]^{1/2} \tag{18}$$

From the Equation (18), overall uncertainty in calculation of $\varepsilon_{wb}$ is found as 6.51%.

The uncertainty rate evaluated for different parameters are presented in Table 3.

***Table 3.*** *Evaluated uncertainty for various parameters*

| Parameter | Uncertainty Rate (%) |
|---|---|
| $\dot{Q}_C$ | 4.53 |
| $\dot{Q}_{solar,g}$ | 2.16 |
| $\dot{Q}_{useful,Hx}$ | 5.83 |
| $\dot{Q}_{trans,des}$ | 6.14 |
| $\varepsilon_{wb}$ | 6.51 |
| $\varepsilon_d$ | 2.41 |
| $\eta_{collector}$ | 2.37 |
| $\eta_{ch}$ | 5.73 |
| $\eta_{hyg}$ | 2.82 |
| $COP_{th}$ | 5.44 |
| $COP_t$ | 5.5 |

## 3. RESULTS AND DISCUSSIONS

In this section, three cycles (charging/discharging) testing results of the investigated SD-SDAEC system were presented. Based on the obtained data through measurements, several performance parameters were analyzed and obtained results are presented below.

### 3.1. Charging Cycle Analysis

The variation of the intensity of solar radiation during the charging tests is shown in Figure 3. The charging performance depends heavily on the solar radiation absorbed by the system. The solar irradiance measurements were performed every 20 minutes. The average of the solar irradiance for the three charging cycles was 842, 822, and 789 W/m$^2$. Each cycle was completed in six hours.

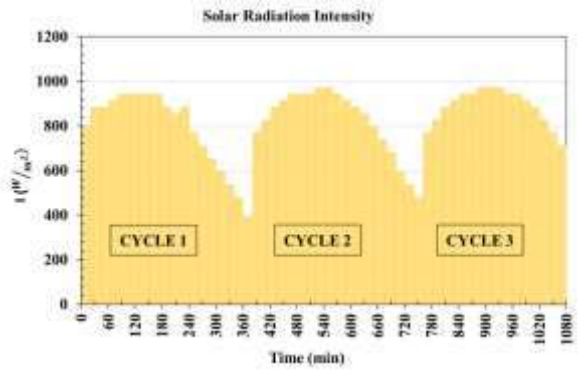


***Figure 3.*** *Variation in the intensity of solar radiation entering the flat plate solar collector*

A seen in Figure 4(a), collector outlet water temperature for all cycles was in the range of 75 – 85 ºC, while the desiccant inlet temperature varied between 57.5 °C – 66.1 °C, 54.1 °C – 60.1 °C and 46.3 °C – 55.4 °C for different testing days. In charging cycles, flow rate of air is selected as 0.03 kg/s, to enable ambient air to reach to the desired temperature required for regeneration.

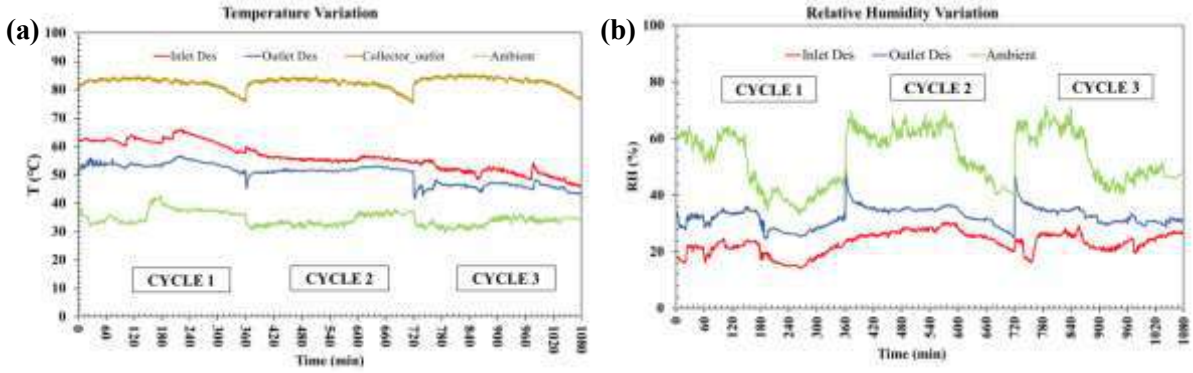


***Figure 4.*** *(a) Variation of temperature, (b) RH of air in charging cycle*

Figure 4 (b) illustrates the air relative humidity changes through the process components. As the air temperature increases at the inlet of desiccator, its relative humidity drops to a level between 15-30%, while at the desiccant outlet it increases to 30-40%. Based on the calculated air absolute humidities, average water desorption rate from the desiccant was found 3.53, 3.48 and 3.43 g/min in different tests.

The variation of the available solar energy that radiated to the flat plate solar collector during the charging cycle is shown in Figure 5. The average of the input solar energy for the three cycles is 1.44, 1.42, and 1.38 kW, respectively.

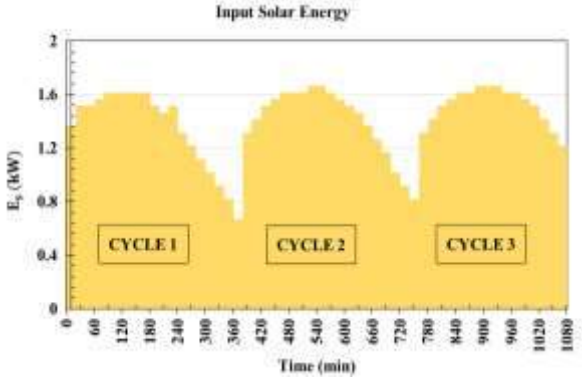


***Figure 5.*** *Variation of the input solar energy*

The average values of available solar energy on collector surface ($Q_{solar,\ ava}$), the rate of heat gain of solar collector ($Q_{solar,g}$), heat transfer rate to the air across the AW-HEX ($Q_{useful,Hx}$), and heat transfer rate to the desiccant for moisture desorption ($Q_{trans,des}$) in charging cycles are illustrated in Figure 6. As shown, the average available solar radiation on the collector surface was 1.43 kW, whereas 0.67 kW of it is gained by the collector during the experiments. Furthermore, the rate of heat transfer to the charging air was found 0.59 kW, which indicates that the heat transfer across the heat exchanger was effective. Finally, results showed that the rate of heat consumption for moisture desorption was 0.16 kW, which was lower than the desired heat transfer ratio. The low desorption heat consumption could be due to the relatively low regeneration temperature used in charging < 65 °C. Additionally, desiccant bed thickness and charging $\dot{m}_a$ might influence desorption heat consumption, thereby, increasing the bed thickness and $\dot{m}_a$ could enhance the heat transfer rate across the desiccant bed. Such improvements could be considered in future studies.

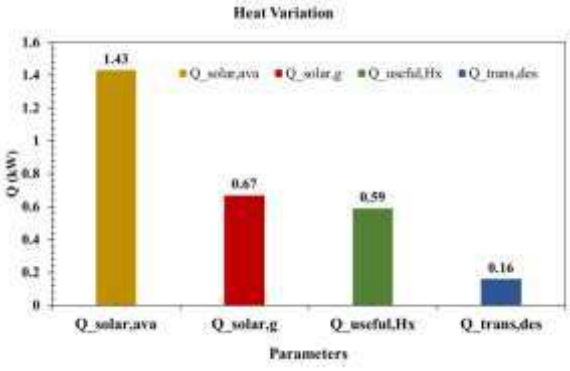


***Figure 6.*** *The average heat variation across the system*

By calculating the energy break-down across the system components (Eqs. 8-9 and 14-15), cyclic $\eta_{collector}$ and $\eta_{ch}$ were determined (Eqs. 10 and 16) and presented in Figure 7. Here, $\eta_{collector}$ is defined as the ratio of $Q_{solar,g}$ to $Q_{solar,ava}$, whereas charging efficiency is the ratio of $Q_{trans,des}$ to $Q_{solar,g}$. Accordingly, $\eta_{collector}$ and $\eta_{ch}$ were found in the range of 0.51-0.46 and 0.27-0.22 respectively. For both efficiencies, a slight drop is observed over the repeating cycles. This could be mainly due to the gradually decreasing $Q_{solar,\ ava}$ over the cycles. As a result, $Q_{solar,g}$ and $Q_{trans,des}$ were decreased, which negatively influenced the $\eta_{collector}$ and $\eta_{ch}$. In addition, some residual moisture remained inside the desiccant over the repeating charging cycles might have affected the heat transfer rate in desiccant chamber. Modifications in desiccant bed configuration could be considered for enhancing the $\eta_{ch}$.

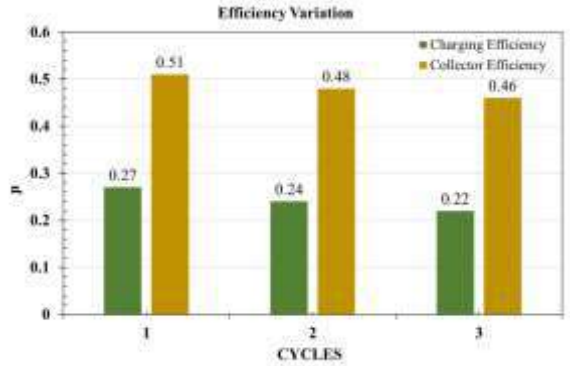


***Figure 7.*** *Collector efficiency and charging efficiency of the SD-SDAEC system*

### 3.2. Discharging Cycle Analysis

Performance of the developed system for the three discharging cycles has been discussed in this section. Each cycle was completed in four hours. Figure 8(a) illustrates the temperature of air at different points of the process. System inlet and outlet temperatures were obtained in the range of 32-35 ° and 24-26 °C respectively. As can be seen in the figure, average temperature difference between desiccant inlet and evaporative cooling chamber outlet was about 7.4 °C, 7.6 °C and 7.9 °C respectively. The variation of the relative humidity at various points of the system is shown in Figure 8(b). Relative humidity at the desiccant inlet was in the range of 49– 65% for different cycles whereas at the outlet of the desiccant chamber it changed from 34% to 53%. The reason of this reduction is because of the water absorption of desiccant material. The relative humidity at the outlet of the heat exchanger and EC chamber was varying between 41-62% and 85-95% respectively.

In the system excess heat produced during desiccation is eliminated by transferring it to an external water tank. As illustrated in 6a, there is between 4-6 °C temperature drop across the heat exchanger (Outlet Des - HX outlet), illustrating the pre-cooling process of air prior to entering the EC chamber. The rate of the heat rejected to water in four hours was determined as 0.29, 0.24, and 0.32 kW, respectively (Please see:

Figure 8c). By rejecting heat to the tank, the temperature of the processed air temperature decreases close to the ambient (desiccant inlet) temperature (Please see: Figure 4a), which consequently can increase the efficiency of the system.

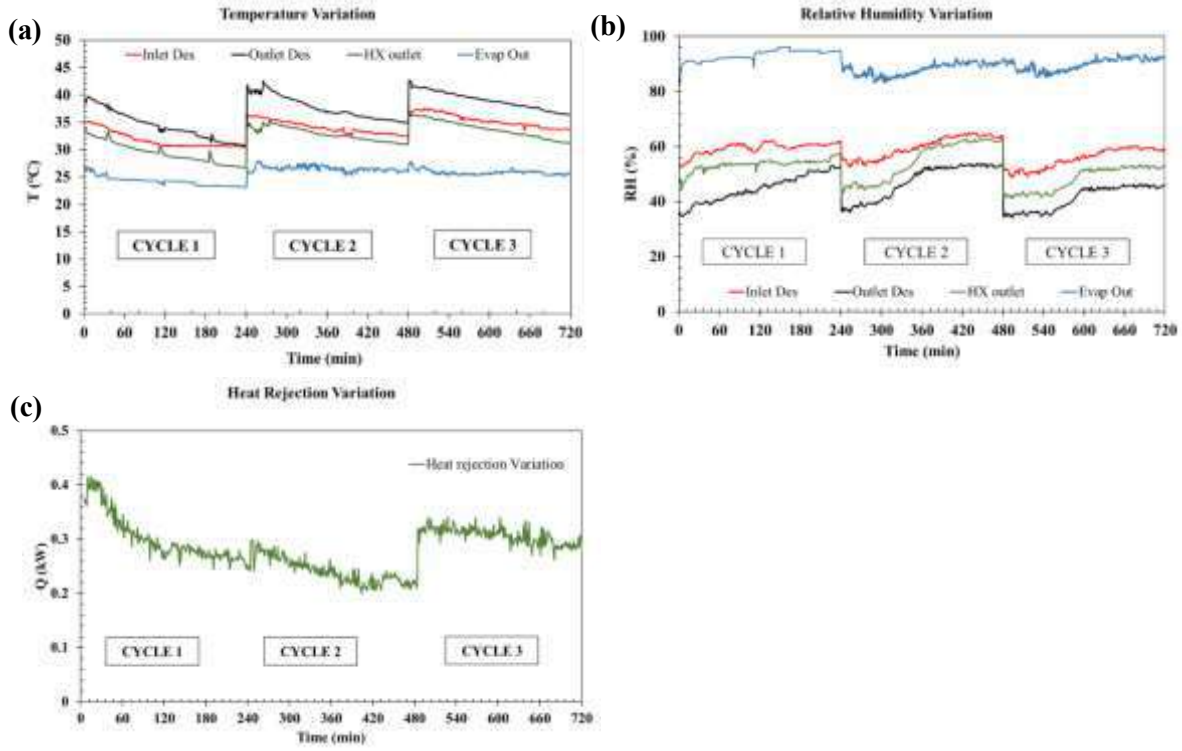


***Figure 8.*** *Variation of (a) temperature, (b) RH of air and (c) heat rejection variation in discharging cycles*

Figure 9(a) presents the wet-bulb effectiveness values of the process. The peak values were obtained as 134%, 131% and 130% in different tests, demonstrating the high performance of the system, where sub wet bulb temperatures were achieved. The dew-point effectiveness variation in discharging mode was demonstrated in Figure 9(b). As it is clear from figure, in the discharging process the first cycle provided dew-point effectiveness flactuating between 73-95%, whereas in the second cycle values were in the range of 85-95%. The third cycle was in the range of 84-96%. The average dew point effectiveness for three cycles was ~90%, which demonstrated that the investigated process has good performance under real climate conditions.

The cooling rate variation in the discharging mode is presented in Figure 9(c). The cycles demonstrated a similar behavior with maximum cooling capacity of 0.73 kW, which was obtained in the third cycle. The average $Q_c$ values were determined as 0.45 kW, 0.47 kW and 0.57 kW respectively. The reason of higher average $Q_c$ in third cycle was the higher temperature and lower relative humidity of ambient air during that cycle. The average ambient temperature and relative humidity were 31.7 °C, 34.0 °C, 35.2 °C and 59.4%, 57.8%, 55.6% over the repeating cycles. Accordingly it could be stated that; beside the design and configuration of the system, the ambient conditions also significantly influences the SD-SDAEC performance. The higher ambient temperature and lower ambient relative humidity could enhance the cooling capacity as a result higher cooling performance could be achieved.

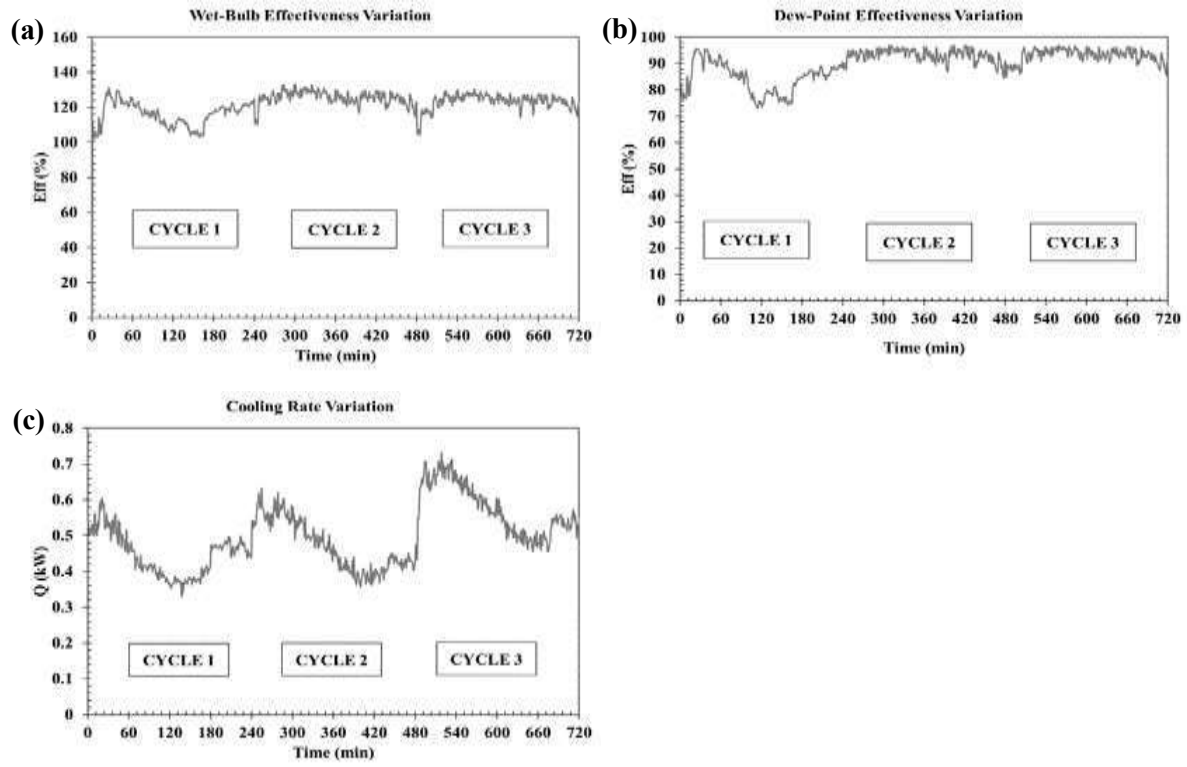


***Figure 9.*** *Variation of (a) wet-bulb effectiveness, (b) dew-point effectiveness and (c) cooling rate*

### 3.3. Overall Performance Analysis

Figure 10(a-b) shows the rate of water absorption/desorption in different experiments. Average values are calculated as 9.64/4.24, 9.19/3.89 and 8.5/3.81 g/min for the cycle order of 1→3. In that regard, total amount of water loaded and removed from the desiccant were calculated as 2314.70/1529.13, 2206.12/1403.46, and 2041.41/1392.02 g for the same order of cycles (Please see: Figure 10(c)). It is also found that, with the decline of average charging temperature from 62 °C to 51 °C, the amount of moisture desorption was reduced. Therefore, it is suggested to increase the $T_{reg}$ in order to rise the cyclic efficiency of the system. Also it is recommended to use more efficient solar collector, and/or an auxiliary heater driven with photovoltaics, although it will increase the cost of the system and affect the feasibility of the system.

The obtained values of the other important performance parameters, $COP_{th}$ and $COP_t$, are given in Figure 10(d). Results showed that, both $COP_{th}$ and $COP_t$ showed an increasing trend from the first to third cycles. As discussed before, higher $Q_c$ values were obtained over the repeating cycles due to the increase in ambient temperature and decrease in ambient humidity. Additionally, $Q_{trans,Hx}$ dropped over the repeating cycles due to the decreased solar radiation. As $COP_{th}$ and $COP_t$ are directly proportional with $Q_c$ and indirectly proportional to $Q_{trans,Hx}$, both of them showed a gradual increase over the repeating cycles. Accordingly, $COP_{th}$ varied in the range of 0.39→0.86 whereas $COP_t$ was between 0.26→0.46. The overall average $COP_{th}$ and $COP_t$ were calculated as 0.6 and 0.35 respectively. Table 4 represents summary of the present study in comparison with the previous studies in the literature.

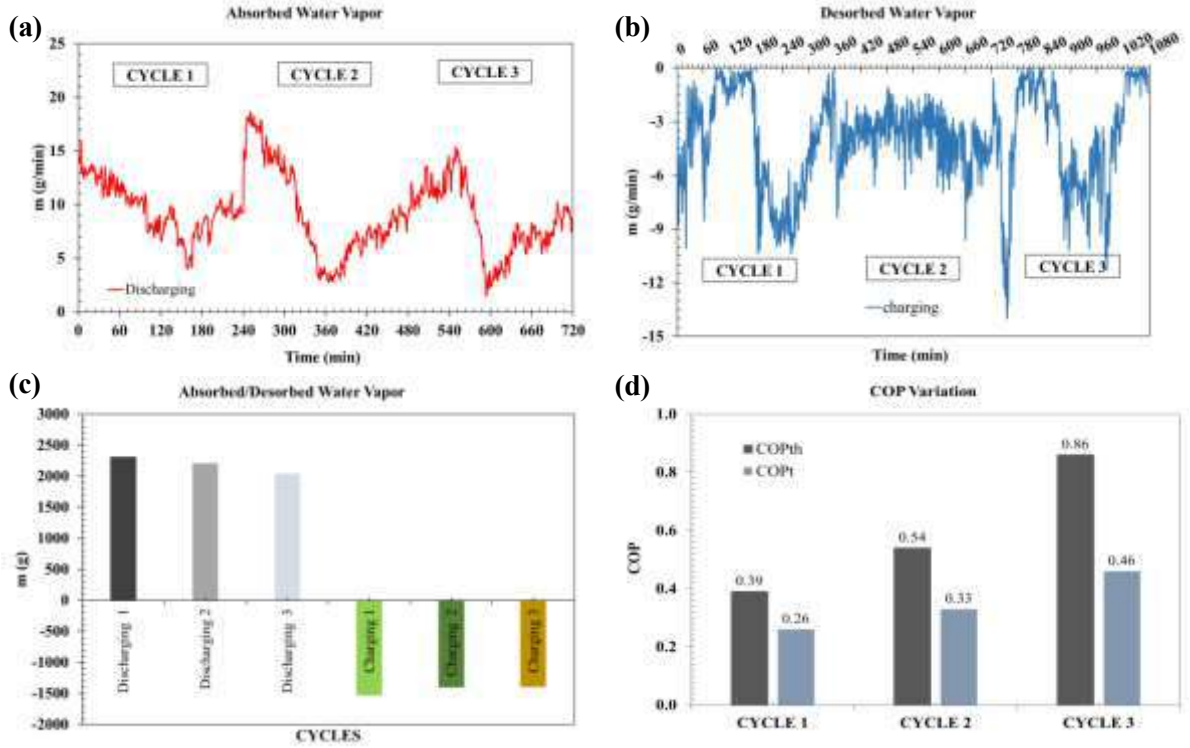


***Figure 10.*** *(a) Rate of water (a) absorption (b) desorption, (c) cumulative moisture absorption / desorption, (d) COP variation*

***Table 4.*** *Summary of the related studies*

| Reference | Year | Type of study | System Performance | Advantages | Disadvantages |
|---|---|---|---|---|---|
| Heidari et al. [16] | 2019 | Num. | $COP_{avg}$ of the proposed system was 1.53. | Good potential for coproduction of water and cooling in hot and humid climates. | Water production capacity of the system is limited |
| Lee et al. [3] | 2020 | Exp. And Num. | In DAEC mode maximum COPth of 0.23 was achieved. | System does not use refrigerant and compressor. | System performance was lower than vapor compression assisted desiccant system |
| Kousar et al. [15] | 2021 | Exp.and Num. | COP of 0.76 is achieved (in direct EC mode) | Provides energy savings >50% compared to conventional A/Cs | Complex system design. Also payback period is >5 years |
| Belguith et al. [8] | 2021 | Num. | COP of 1.89 was achieved. | Efficient in ventilation mode | System performance decreases with the increase of ambient humidity. |
| Present study | 2021 | Exp. | In DAEC mode maximum $COP_{th}$ of 0.86 was achieved. | System uses low cost desiccant and ECPMs. It has simple configuration and provides high effectiveness. | Not suitable for continuous operation. |

### 3.4. Potential Real-Life Application of SD-SDAEC System

In this section, a potential low-cost implementation method of the investigated SD-SDAEC system in real building applications is presented. For that purpose, the case of Northern Cyprus (NC) is considered. In NC, nearly all buildings are equipped with flat plate solar collector systems for hot water production (Please see: Figure 11).

The schematic view of the investigated storage type SD-SDAEC unit, illustrating its operational modes, is given in Figure 11. The proposed concept consists of solar water heating system, a desiccant chamber, and the evaporative cooling chamber. Also hot and cold heat exchangers are used for transferring solar heat to the air in the charging cycle and rejecting sorption heat from the air in discharging cycle. As seen from the figure, in charging mode (Figure 11b), water from the hot water tank is circulated across the heating coil, and the air is heated. Hot air passes across the desiccant and desorbs the moisture. Moist air is then exhausted to the environment through the exhaust outlet. In discharging mode (Figure 11a), water circulation from the hot water tank is deactivated. Therefore, air passes across the heating coil without any heat transfer. Then it enters the desiccant chamber where the moisture is absorbed, and air humidity content is reduced. Following that, air passes across the pre-cooling heat exchanger, which is connected to the cold water storage tank. In this way, generated sorption heat is rejected to the cold water tank, and the temperature of the air is dropped to the ambient level. Finally, air enters the EC chamber, where its temperature is reduced to 22-25 °C. Product air is then supplied to the building. As the solar water heating system already exists in the majority of buildings, the installation costs of the system are expected to be low (1000-1500 €). Implementation of such a system could provide a low-cost and sustainable opportunity for reducing the indoor temperature in buildings.

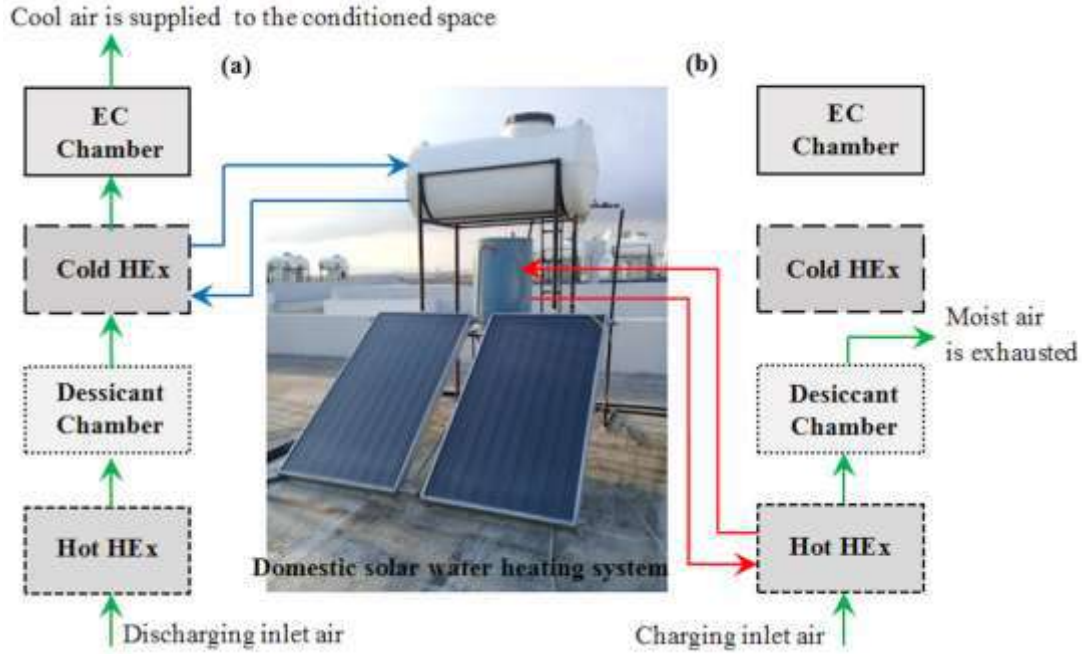


***Figure 11**: Schematic illustration of; (a) discharging process, (b) charging process of the storage type SD-SDAEC system in residential buildings (Photo is taken by authors)*

## 4. CONCLUSIONS

The performance of the new storage type SD-SDAEC system developed in the present work was examined under NC climatic conditions. Based on the analysis results, the important conclusions are listed below:

- Three discharging- charging cycles, utilizing Vmc-$CaCl_2$ as the desiccant material and wood chips as the evaporation material, were conducted in the developed SD-SDAEC system. Over six hours of charging at $T_{reg}$ = 62 – 51 °C and $\dot{m}$= 0.03 kg/s, in charging mode operation, average moisture desorption rate of 3.9 g/min was achieved.
- Over four hours of discharging at $T_i$ = 32 – 35 °C and $\dot{m}$= 0.06 kg/s, $\Delta T_{ave}$ and $\dot{Q}_{c,ave}$ of 8.4 °C and 0.49 kW were achieved.
- System's $\varepsilon_{wb,ave}$ and $\varepsilon_{d,ave}$ were determined as 121.6% and 90.2%, respectively.
- With the drop of charging temperature from 62 °C to 51 °C, water removal capacity drop between 1529.13 g and 1392.02 g.

- Average value of $\eta_{hyg}$ was obtained between 0.63-0.68 in different cycles.
- The $COP_{th,ave}$ and $COP_{t,ave}$ of the system were determined as 0.6 and 0.35.

As presented above, encouraging results were achieved from the real life testing of the investigated novel storage type SD-SDAEC system. Such configuration could be useful in buildings for storing solar radiation in the form of coolth energy. As a result, dependency on fossil fuel sourced cooling systems could be reduced. An important advantage of the investigated technology is its suitability for integration with existing solar collectors in buildings. This could ease the implementation of SD-SDAEC system while reducing the capital costs. However further research is required for improving material properties and heat/mass transfer effectiveness across the system components also optimizing the operating conditions.

## REFERENCES

[1] Farooq, A. S., Badar, A. W., Sajid, M. B., Fatima, M., Zahra, A., Siddiqui M. S. (2020). Dynamic simulation and parametric analysis of solar assisted desiccant cooling system with three configuration schemes. Solar Energy, 197, 22-37.

[2] Comino, F., González, J. C., Navas-Martos, F. J., de Adana, M. R. (2020). Experimental energy performance assessment of a solar desiccant cooling system in Southern Europe climates. Applied Thermal Engineering, 165, 114579.

[3] Lee, Y., Park, S., Kang, S. (2021). Performance analysis of a solid desiccant cooling system for a residential air conditioning system. Applied Thermal Engineering, 182, 116091.

[4] Jagirdar, M., Lee, P. S., Padding, J. T. (2021). Performance of an internally cooled and heated desiccant-coated heat and mass exchanger: Effectiveness criteria and design methodology. Applied Thermal Engineering, 188, 116593.

[5] Jia, C. X., Dai, Y. J., Wu, J. Y., Wang, R. Z. (2006). Analysis on a hybrid desiccant air-conditioning system. Applied Thermal Engineering, 26(17-18), 2393-2400.

[6] Asim, N., Amin, M. H., Alghoul, M. A., Badiei, M., Mohammad, M., Gasaymeh, S.S., ... Sopian K. (2019). Key factors of desiccant-based cooling systems: Materials. Applied Thermal Engineering, 159, 113946.

[7] Jani, D. B., Mishra, M., Sahoo, P. K. (2015). Performance studies of hybrid solid desiccant–vapor compression air-conditioning system for hot and humid climates. Energy and Buildings, 102, 284-292.

[8] Belguith, S., Meddeb, Z., Slama, R. B. (2021). Performance analysis of desiccant cooling systems in a hot and dry climate. Euro-Mediterranean Journal for Environmental Integration, 6(1), 1-11.

[9] Aoul, K. A. T., Hasan, A., Dakheel, J. A. (2021). Assessment of solar dehumidification systems in a hot climate. Sustainability, 13(1), 277.

[10] De Antonellis, S., Colombo, L., Freni, A., Joppolo, C. (2021). Feasibility study of a desiccant packed bed system for air humidification. Energy, 214, 119002.

[11] Hussain, S., Kalendar, A., Rafique, M. Z., Oosthuizen, P. (2020). Numerical investigations of solar-assisted hybrid desiccant evaporative cooling system for hot and humid climate. Advances in Mechanical Engineering, 12(6), 1-16.

[12] Bleibel, N., Ismail, N., Ghaddar, N., Ghali, N. (2020). Solar-assisted desiccant dehumidification system to improve performance of evaporatively cooled window in hot and -humid climates. Applied Thermal Engineering, 179, 115726.

[13] Pandelidis, D., Pacak, A., Cichoń, A., Anisimov, S., Drąg, P., Vager, B., & Vasilijev, V. (2018). Multi-stage desiccant cooling system for moderate climate. Energy Conversion and Management, 177, 77-90.

[14] Riaz, F., Qyyum, M. A., Bokhari, A., Klemeš, J. J., Usman, M., Asim, M., ... & Lee, M. (2021). Design and energy analysis of a solar desiccant evaporative cooling system with built-In daily energy storage. Energies, 14(9), 2429.

[15] Kousar, R., Ali, M., Sheikh, N. A., Gilani, S. I. ul H. (2021). Holistic integration of multi-stage dew point counter flow indirect evaporative cooler with the solar-assisted desiccant cooling system: A techno-economic evaluation. Energy for Sustainable Development, 62, 163-174.

[16] Heidari, A., Roshandel, R., & Vakiloroaya, V. (2019). An innovative solar assisted desiccant-based evaporative cooling system for co-production of water and cooling in hot and humid climates. Energy Conversion and Management, 185, 396-409.

[17] Avargani, V. M., Karimi, R., & Gheinani, T. T. (2019). Mathematical modeling of an integrated system for regeneration of solid desiccants using a solar parabolic dish concentrator. International Journal of Heat and Mass Transfer, 142, 118479.

[18] Khosravi, N., Aydin, D., Karim Nejhad, M., Dogramaci, P. A. (2020). Comparative performance analysis of direct and desiccant assisted evaporative cooling systems using novel candidate materials. Energy Conversion and Management, 221, 113167.

[19] Cengel, Y. A., Boles, M. A., (2007). Thermodynamics: An Engineering Approach. 6th Editon (SI Units) New York, NY, USA: The McGraw-Hill Companies, Inc.

[20] Introduction to Humidity: Basic Principles on Physics of Water Vapor, Retrieved from: https://www.soselectronic.com/a_info/resource/c/sensirion/Sensirion_Introduction_to_Relative_Humidity_V2.pdf Access date: 10th May 2021.

[21] Cao, Z., Tester, J. W., Sparks, K. A., Trout, B. L. (2001). Molecular computations using robust hydrocarbon− water potentials for predicting gas hydrate phase equilibria. The Journal of Physical Chemistry B, 105(44), 10950-10960.

[22] Sonntag, R. E., Van Wylen, G. J., Borgnakke, C. (2008). Fundamentals of Thermodynamics. 8th ed. New York, NY, USA: Wiley.

[23] Buker, M. S., Mempouo, B., Riffat, S. B. (2014). Performance evaluation and techno-economic analysis of a novel building integrated PV/T roof collector: An experimental validation. Energy and Buildings, 76, 164-175.

[24] Jani, D. B., Mishra, M., Sahoo, P. K. (2018). Investigations on effect of operational conditions on performance of solid desiccant based hybrid cooling system in hot and humid climate. Thermal Science and Engineering Progress, 7, 76-86.